Journal of Photochemistry and Photobiology A: Chemistry 353 (2018) 536–545

Contents lists available at ScienceDirect

Journal of Photochemistry and Photobiology A: Chemistry

journal homepage: www.elsevier.com/locate/jphotochem

Singlet oxygen production by a polypyridine ruthenium (II) complex with a perylene monoimide derivative: A strategy for photodynamic inactivation of *Candida albicans*

Paulo José Sousa Maia[a,b,d,*], Inara de Aguiar[b], Marisol dos Santos Velloso[c], Dong Zhang[d], Edjane Rocha dos Santos[b], Jonatas Rafael de Oliveira[c], Juliana Campos Junqueira[c], Matthias Selke[d,**], Rose Maria Carlos[b]

[a] *Institute of Exact Sciences and Technology, Federal University of Amazonas, 69103-128, Itacoatiara, AM, Brazil*
[b] *Department of Chemistry, Universidade Federal de São Carlos, CP 676, 13565-905, São Carlos, SP, Brazil*
[c] *Department of Biosciences and Oral Diagnosis, Universidade Estadual Paulista/UNESP, Av. Engenheiro Francisco José Longo, 777, 12245-000, São José dos Campos, SP, Brazil*
[d] *Department of Chemistry and Biochemistry, California State University, 90032, Los Angeles, CA, United States*

ARTICLE INFO

Article history:
Received 16 November 2017
Received in revised form 10 December 2017
Accepted 12 December 2017
Available online 13 December 2017

Keywords:
Singlet oxygen
Photodynamic therapy (PDT)
Candida albicans
Ruthenium polypyridine complex
Photoluminescence

ABSTRACT

We report the synthesis, optical, electrochemical and electronic properties of a new perylene derivative and its Ru(II) complex, namely N,-(5-amino-1,10-phenantroline)perylene-3,4,9,10-tetracarboximonoimide (pPDI) and Bis(1,10-phenanthroline)(N-(5-amin-1,10-phenantroline)perylene-3,4,9,10-tetracarboxi monoimide)ruthenium(II) hexafluorophosphate, $[Ru(phen)_2(pPDI)]^{2+}$ $([PF_6]^-)_2$. The molecular structures of the compounds were elucidated by FTIR, mass spectrometry, elemental analysis (CHN) and DFT calculations. Their optical and electrochemical properties were investigated by absorption and fluorescence spectroscopy and cyclic voltammetry. The spectroscopic and electrochemical studies for both the pPDI and the perylene monoimide metal complex show that Ru^{2+} coordination does not affect the optical and electrochemical properties of the free perylene bisimide ligand. The Ru complex exhibits emission lifetimes of 5.06 ns (48.1%) and 156 ns (51.9%), resulting from emission of the pPDI ligand and ^{3}MLCT, respectively. The pPDI triplet excited state in the title chromophore is able to sensitize the production of singlet oxygen ($^1O_2$). Using a time-resolved laser system, we measured the quantum yield for the production of singlet oxygen ($\Phi\Delta$) to be 0.26 for *cis*-$[Ru(phen)_2(pPDI)]^{2+}$. *Candida albicans* is recognized as the most common fungal pathogens, causing superficial infections of the skin and mucous membranes. Resistance of *C. albicans* strains against classical antifungal agents such as fluconazole has increased considerably, which drives the search for new therapeutic alternatives. In the present study, we report that our new Ru-perylene complex can indeed be used to kill the bacterium *C. albicans*. The fungicidal activity of *cis*-$[Ru(phen)_2(pPDI)]^{2+}$ against *C. albicans* was evaluated in the presence of *C. albicans* cultures in the dark and in the presence of light. After exposure to 12.5 μM of *cis*-$[Ru(phen)_2(pPDI)]^2$ in the presence of light for 180 s, *C. albicans* showed a decrease of 50% in its concentration compared to the same experimental conditions in the dark.

1. Introduction

Singlet oxygen ($^1O_2$, $^1\Delta_g$), the lowest excited state of the dioxygen molecule, can be generated by photochemical and chemical processes [1–6]. The most common photochemical method involves energy transfer from a triplet excited photosensitizer (^{3}*PS). Many dyes, including some diimides [2–4] and metal complexes[3–10] can be used as photosensitizers for the production of $^1O_2$.

A variety of transition metal complexes have been studied as photosensitizers for singlet oxygen generation [2,5–8]. Amongst these complexes, Ru(II)-polypiridyl complexes have been investigated due to their stability, inertness and biological activity [7–10]. These complexes have long emission lifetimes from the triplet

* Corresponding author at: Department of Chemistry, Universidade Federal de São Carlos, CP 676, 13565-905, São Carlos, SP, Brazil.
** Corresponding author.
E-mail addresses: pmldcb@gmail.com (P.J.S. Maia), mselke@calstatela.edu (M. Selke).

https://doi.org/10.1016/j.jphotochem.2017.12.020
1010-6030/

metal-to-ligand charge transfer state (^{3}MLCT) ($d\pi \rightarrow \pi^*$, α-diimine states) [11]. This state is rapidly quenched by triplet (ground state) dioxygen, which makes many Ru(II)-polypiridyl complexes both efficient oxygen sensors and singlet oxygen sensitizers [7–10,12]. For example, Demas and co-workers analyzed the oxygen quenching by Ru (II), Os (II) and Ir (III) polypiridyl complexes containing bipyridine, 1,10-phenanthroline and/or phenanthroline diimines [8,13]. These complexes have shown high quantum yields for singlet oxygen formation, with values of $\Phi\Delta$ ranging from 0.68-0.86.

Upon excitation of Ru(II) complexes, singlet excited states of the ligand and the ^{1}MLCT state $d_{Ru} \rightarrow \pi^*_L$ are initially formed. From these states, intersystem crossing to the ^{3}MLCT state takes place, which is responsible for the luminescence of Ru(II) complexes. Therefore, to modulate and increase the absorption and emission properties of Ru(II) complexes, molecular engineering of its ligands has been attempted [14].

However, Ru complexes with mixed ligands showed much lower triplet lifetimes. This is due to the increase in conjugation, which results in the availability of lower excited state energy levels for non-radiative deactivation of the ^{3}MLCT state. Complexes where the ligand is substituted with an aryl group in the 5-position were found to have longer excited-state lifetimes and were the most efficient photosensitizers [15]. Substituted ethoxybenzene or vinyl-linked benzocrown-ether-2,2-bipyridine Ru(II) complexes have also been tested for their singlet oxygen production ability, and their quantum yields are in the range of 0.18–0.47 [13]. A series of aza-15-crown-5-vinyl-2,2-bipyridine Ru(II) complexes and multinuclear Ru(II) complexes were investigated by Abdel-Shafi et al. and these polypyridine complexes had quantum yields that ranged from 0.21 to 0.54 [13].

For many large-scale photochemical processes, it would be desirable to employ photosensitizers that show strong absorption of radiation in the visible region, ideally near the solar maximum. The absorption spectra of the perylene complexes, in general, do show a high absorption coefficient in the visible region. Thus, such complexes could potentially be used for photochemical processes initiated by sunlight. This might include generation of singlet oxygen, and subsequent pollutant degradation and photodynamic activity [7,10,15]. A number of perylene-3,4,9,10-tetracarboxylic acid (diimide) derivatives, known as PDIs, and polypyridine complexes derived from perylenes have shown good results in the production of reactive species of reactive oxygen species (ROS) [11,16–18]. The ligands containing the perylene moiety are reddish dyes with very high quantum yields of luminescence. However, an undesired property of perylene complexes is the formation of molecular aggregates, which is facilitated by the flatness of the perylene molecules [19,20].

The perylene dyes are known for their poor solubility in organic solvents (typically 1–2 mg L^{-1}) [11,21,22]. Their PDI diimide derivatives with symmetrical and unsymmetrical secondary, or tertiary alkyl side chains N,N'-bis(1-isobutyl-3 methylbutyl) perylene-3,4:9,10-bis(dicarboximide), N,N'-bis(1-butylhexyl)perylene-3,4:9,10-bis(dicarboximide) and N,N'-bis(5-*tert*-butyl-1,3,4-thiadiazole-2-yl)perylene-3,4:9, 10-bis(dicarboximide) were synthesized and had significantly improved solubility (10 mg/mL) in dichloromethane, chloroform, ether, hexane, chlorobenzene and toluene [16,17]. Single or double amine substitution on the perylene core can also lead to a red shift of the absorption maximum up to 750 nm [11,22,23].

Recently, Santos and co-wokers [11] synthesized the complex *cis*-[(phen)2Ru(pPDIp)]2+, where pPDIp is a perylene diimine group functionalized with phenanthroline ligands where one side is coordinated to a Ru(II) center. The complex shows strong electronic absorption bands attributed to the pPDIp and $\{Ru(phen)_2\}^{2+}$ moieties in acetonitrile. The charge-separated intermediate species decays to generate the triplet state ^{3*}pPDIpRu(II) ($\tau P = 1.8$ μs) that sensitizes the formation of singlet molecular oxygen with quantum yield $\Phi_\Delta = 0.57$. The electronic coupling between the pPDI ligand and the Ru(II)-polypyridine unit was assigned to allow the population of the triplet ^{3*}PDI excited states from the ^{3*}MLCT emitter state, generating an excited state $\{(Phen)_2Ru^{3+}(PPDIp^{\bullet-})\}$. It is important to note that the rigid structure of the complex unit $\{Ru(phen)_3\}^{2+}$ with strong coordination of the ligand field leads to the stability of the complex avoiding its photodissociation. These studies exemplify how molecular engineering of the ligands is relevant to be used to modulate the photophysical behavior of the ligands coordinated to the Ru(II).

The high extinction coefficients, ease of triplet formation, and absorption in the visible range make the perylene complexes good candidates for singlet oxygen sensitizers. Given their high extinction coefficients in the visible range, they can be potentially used as candidates in the field of photodynamic inactivation of microorganisms, against cancer cells and pathogenic microorganisms. Several groups have investigated Ru(II) complexes for their photodynamic activity. Akkaya et al. have synthesized a series of water-soluble green perylenediimide (PDI) dyes. Upon excitation with red light, these dyes were shown to be efficient generators of singlet oxygen, and in cell culture media, they were shown to display significant light-induced cytotoxic effects on the human erythroleukemia cell line (K-562) [24].

In the present study, we prepared a new polypyridine complex of ruthenium *cis*-$[Ru(phen)_2(pPDI)]^{2+}$, where pPDI is a perylene group monoimide functionalized in one of the coordinated phenanthroline ligands (Fig. 1). Our strategy is to keep the tris-chelate structure around the Ru(II) metal center using the complex

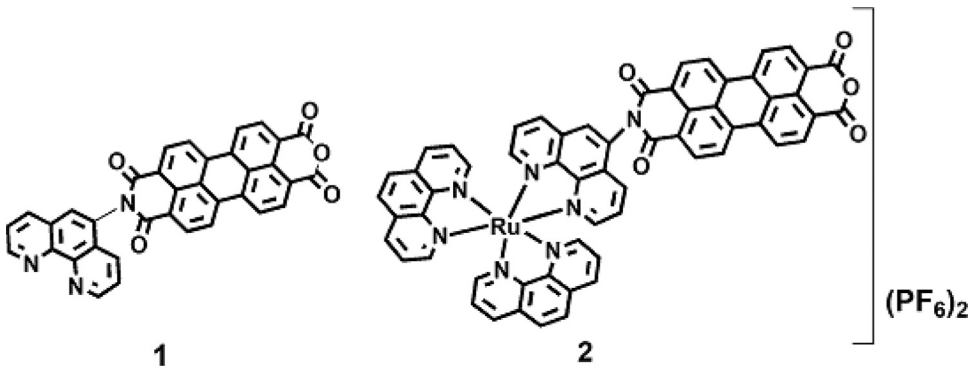

Fig. 1. Representative structures of N,-(5-amin-1,10-phenanthroline)perylene-3,4,9,10-tetracarboximonoimide (pPDI)-(1) [22] and Bis(1,10-phenanthroline)(N-(5-amin-1,10-phenantroline)perylene-3,4,9,10-tetracarboximonoimide)ruthenium(II) hexafluorophosphate, *cis*-Ru(pPDI)($phen_2$])$(PF_6)_2$-(2).

$[Ru(phen)_3]^{2+}$ so as to improve the stability of the complex in question and to ensure strong absorption to the ^{1*}MLCT state. This state should rapidly decay to populate ^{3*}MLCT which may subsequently sensitize the formation of singlet oxygen. In addition, we expect that the compound solubility will increase after coordination to the metal ion.

One of the most important clinical pathogenic microorganisms is *Candida albicans* due to its remarkable virulence. *C. albicans* is recognized as the most common fungal pathogens, causing superficial infections of the skin and mucous membranes, reaching systemic levels, especially in immune-compromised individuals [25,26]. The resistance of *C. albicans* strains against classical antifungal agents such as fluconazole has increased considerably, which drives the search for new therapeutic alternatives [27–29]. In the present study, we report that our new Ru-perylene complex can indeed be used to kill the bacterium *C. albicans.*

2. Experimental

2.1. Materials, spectroscopic measurements, and characterization

Perylene-3,4,9,10-tetracarboxylic dianhydride, $RuCl_3 \times H_2O$, 1,10-phenanthroline (phen), zinc acetate, lithium chloride and tetrabutylammonium hexafluorophosphate were obtained from Aldrich. HPLC grade solvents were distilled just before being used in the spectroscopies experiments.

The complex *cis*-$[Ru(phen)_2(H_2O)_2](PF_6)_2$ was prepared according to the procedures described in the literature [30,31]. The synthesis, electrochemical and spectroscopic experiments were conducted under nitrogen atmosphere.

The CHN elemental analysis of pPDI and *cis*-$[Ru(phen)_2(pPDI)](PF_6)_2$ complex was performed on an EA 1110 CHNS-O Carlo Erba Instrument. FTIR spectra were recorded on a Bomem-Michelson 102 spectrometer in solid state using CsI pellets in the range of $4000 - 300\,cm^{-1}$.

The electronic absorption spectra were recorded on an Agilent 8453A UV–vis spectrophotometer or on a Jasco V-660 UV–vis spectrophotometer. Voltammetric measurements were carried out with a μAutolab Type III potentiostat at 25 °C without light. Glassy carbon electrode as working electrode (d = 2 mm), Pt electrode as counter electrode (d = 4 mm), Ag/AgCl electrode as reference electrode, ferrocene as internal reference electrode and $TBAPF_6$, 0.1 M, as supporting electrolyte. The scan rate was 100 mV/s and the concentration of the acetonitrile solutions that were used to perform cyclic voltammetry measurements of synthesized compounds was $10^{-3}\,mol\,L^{-1}$.

2.1.1. Steady state spectroscopy

The luminescence spectra were recorded on a Shimadzu RF-5301PC spectrofluorometer or on a Horiba Jobin Yvon Fluorolog 3–22 spectrofluorometer. The concentration was $\sim 10^{-5}\,mol\,L^{-1}$ ($\lambda_{absmaximum} = 0.3$), solvent acetonitrile.

2.1.2. Time-resolved photoluminescence

The fluorescence intensity decay curves for the compounds with picosecond resolution were obtained using single photon timing technique with a DCM or Rhodamine dye laser (DCM = 4-(Dicyanomethylene)-2-methyl-6-(4-dimethylaminostyryl)-4H-pyran). Intensity decay measurements were made by a collection of excitation and decay curves, using an emission polarizer set at the magic angle. The excitation profile was recorded at the excitation wavelength with a scattering suspension of the compound being investigated. For the decays, a cut-off filter was used to remove all excitation light. The emission signal passed through a depolarizer, a Jobin Yvon HR-320 monochromator with a grating of 100 lines/mm and was detected with a Hamamatsu 2809U-01 microchannel plate photomultiplier (MCP-PT). The instrument response had an effective FWHM of 35 ps. Fluorescence intensity decay curves were obtained by excitation light at 532 nm using the DCM and Rhodamine laser, with emission collected at 570 nm, respectively. The decay curves were analyzed using home-made non-linear least-square deconvolution software based on the Levenberg–Marquardt algorithm, and the quality of the fit was evaluated by the reduced, the weight residuals and the autocorrelation of the residuals. The intensity of the fluorescence decay curves with nanosecond resolution was obtained on a Fluorolog Horiba Jobin Yvon. Program DataStation V 2.6-Horiba Jobin Yvon S1 Detector HV:950 V, Time Range: 400 ns, Peak Present: 65000 counts, Repetition Rate: 1MHZ, Sync Delay: 50 ns. Fluorescence intensity decay curves were obtained by excitation light at 450 nm using DCM laser with emission collected at 600 nm.

2.1.3. Singlet oxygen detection

The singlet oxygen experiments were performed at room temperature with a Nd-YAG nitrogen laser used for excitation (532 nm, ca. 600 ps pulses, ~1.6 mJ/pulse) with air-equilibrated samples [2]. The emission from singlet oxygen at λ = 1270 nm was detected at 90 ° to the incident laser beam by a 5 MHz germanium photodiode (Judson, J16-8SP-R05M-HS) working at room temperature. We employed several filters, namely a 1270 nm interference filter (*Corion*) or a combination of long-wave pass filters (1000 nm, 1100 nm, 1200 nm, *CVI Laser Corp.*) to reduce scattered radiation from the laser (shortly after the laser pulse). The signal was amplified with a preamplifier (Oriel 70732, 350 MHz and Thorn EMI Electron Tubes A1 and/or A2). Decay curves were obtained with the help of an 8-bit AD-converter/recorder system (Fast TR50; 50 MHz), and each curve was the average of 60 decays. The optical densities at 532 nm were matched for the samples and methylene blue, which was used as the reference compound. The resultant emission curves were fitted with a single-exponential function to obtain the initial luminescence intensity at time t = 0 (or the intensity at any other time t) after the laser pulse. Experiments were done in methanol, acetonitrile, dichloromethane and acetone.

2.1.4. Quantum yield of singlet oxygen

Singlet oxygen quantum yield were determined by direct analysis of its near infrared luminescence intensity in different solvents. Measurements were made with two independent solutions, one containing the molecule under investigation and the other a reference R (R = methylene blue), for which the quantum yield of singlet oxygen is known. The concentrations were adjusted so that the two solutions exhibited identical absorbance at the excitation wavelength [1]. Under these conditions, with identical laser pulse energy, the luminescence intensity ratio is related to the ratio of quantum yields of singlet oxygen production by the two sensitizers. The quantum yield of singlet oxygen was measured in dichloromethane, methanol, acetone, chloroform, and acetonitrile.

2.2. Synthesis and characterization of pPDI and its Ru complex

2.2.1. Synthesis of the ligand phen-perylene (pPDI) N,-(5-amin-1,10-phenanthroline)perylene-3,4,9,10-tetracarboximonoimide

A modified literature procedure [22] was used as follows: one equivalent 136 mg (0.170 mmol) of perylene-3,4,9,10-tetracarboxylic-3,4,9,10-dianhydride (PTCDA) was dispersed in freshly distilled quinoline (10 mL) with one equivalent 32.30 mg (0.170 mmol) of 5-amino-phenanthroline. Next 10% (by weight, relative to 5-amino-phenanthroline) anhydrous zinc acetate was added and the solution was heated under nitrogen to 220 °C for 12 h. After cooling, 15 mL of 1 M HCl was added and the precipitate

was collected and rinsed with water and ether. We then added 150 mL of methanol, stirred for 30 min and allowed the mixture to stand for 4 h at −10° C, followed by washing with a 5% solution of sodium carbonate. After that, the compound was rinsed with methanol and dried under vacuum (50% yield). Insufficient solubility for NMR; The synthesized pPDI (1) was characterized by MALDI-TOF mass spectra with parent molecular ion peaks appearing at $[m/z + 3H^+] = 570.2$ (Fig. S1- Supporting information), which is consistent with the theoretical value of exact mass. Anal. Calcd (found) for pPDI $C_{36}H_{15}N_3O_5$: C, 75.92 (76.36); H, 2.65 (2.92); N, 7.38 (7.32)%.

2.2.2. Synthesis of bis(1,10-phenanthroline)(N-(5-amin-1,10-phenantroline)perylene-3,4,9,10-tetracarboximonoimide)ruthenium (II) hexafluorophosphate, [Ru(pPDI)(phen$_2$)](PF6)2 (2)

The *cis*-[Ru(phen)2(pPDI)](PF6)2 complex was synthesized by reacting *cis*-[Ru(1,10-phen)$_2$(H_2O)$_2$](PF_6)$_2$ [11,30,31] with 1.2 eq. of pPDI in DMF. The complex was isolated as a hexafluorophosphate salt, whose composition and structure were verified by CHN analysis and mass spectrometry, respectively. (65% yield). It was insufficiently soluble for characterization by NMR. The synthesized *cis*-[Ru(phen)2(pPDI)]$^{2+}$ complex was characterized by MS MALDI-TOF mass spectra with parent molecular ion peaks appearing at $[(M-2PF_6)^{+2} = 515.57]$, (Fig. S2- Supporting information), which is consistent with the theoretical value of the exact mass. Anal. Calcd (Found) for $C_{60}H_{31}F_{12}N_7O_5P_2Ru$: C, 69.23 (69.09); H, 2.66 (2.61); N, 10.09 (10.20)

2.3. Biological experiments

Initially, the lowest concentration dosage cytotoxic of photosensitizer *cis*-[Ru(phen)$_2$(pPDI)]$^{2+}$ less cytotoxic was determined by a cytotoxicity test in mouse macrophages and subsequently, the highest concentration of photosensitizer with lower cytotoxicity was used to evaluate the antimicrobial capacity of the photosensitizer against *C. albicans* cells by photodynamic therapy. Cells culture and cytotoxicity tests were performed according to Oliveira et al. [32] with some modifications and the photodynamic therapy was performed according to Freire et al. [33] with modifications.

2.3.1. Photosensitizer solutions

Solutions of the photosensitizer were prepared by dissolving the powder in methanol and sterilized by filtration through a membrane with a pore size of 0.22 μm (MFS, Dublin, CA, USA). After filtration, the photosensitizer solution was stored in the dark.

2.3.2. Cell cultures

Mouse macrophages (RAW 264.7) obtained from the Rio de Janeiro Cell Bank – Associação Técnico Científica Paul Ehrlich (APABCAM – Rio de Janeiro, RJ, Brazil) were cultured routinely in Dulbecco's Modified Eagle Medium (DMEM – LGC Biotechnology, Cotia, SP, Brazil) supplemented with 10% fetal bovine serum (FBS – Gibco, USA) at 37 °C in a 5% CO2 atmosphere. Viable cells were counted by the Trypan blue (0.5%, Sigma-Aldrich, St. Louis, MO, USA) exclusion method.

2.3.3. Cytotoxicity testing (MTT assay)

For the experimental and positive control groups, 40×10^3 viable cells/well were seeded in 96-well plates (Nunc, Kamstrupvej, Roskilde, Denmark) and the plates were incubated for 24 h at 37 °C. Next, the cell cultures were exposed to 200 μL of the serial dilutions of the photosensitizer (100 μM, 50 μM, 25 μM, 12.5 μM and 6.5 μM) and incubated for 5 min. At the end of the exposure, the cell culture medium was discarded and cell survival was determined by the MTT assay [MTT – (3-(4,5-dimethylthiazol-2-yl))-2,5-diphenyltetrazolium bromide; Sigma-Aldrich].

The plates were washed with phosphate-buffered saline (PBS – Cultilab, Campinas, São Paulo, Brazil) and 100 μL MTT solution (0.5 mg/mL in PBS) was added to each well. After incubation for 1 h, MTT solution was removed and 100 μL dimethyl sulfoxide (DMSO – Sigma-Aldrich) was added to each well. The plates were incubated for 10 min and then shaken on a shaker for an additional 10 min. Optical densities were measured in a multi-well spectrophotometer (Bio-Tek, Winooski, Vermont, USA) at 570 nm. The optical density values obtained for cultures exposed to the extracts were normalized to untreated control cultures (corresponding to 100%). The results of the cytotoxicity tests were analyzed by ANOVA and the Tukey test ($P \leq 0.05$) using the BioEstat 5.0 software. The highest concentration of the photosensitizer which was less cytotoxic was selected for the subsequent test.

2.3.4. Photodynamic therapy (PDT) assay on Candida albicans

The *C. albicans* ATCC 18804 strain was seeded onto Sabouraud dextrose agar (Difco, Detroit, USA) and incubated at 37 °C for 48 h. After this period was prepared a standard suspension from the *C. albicans* colonies in physiological solution at a concentration of 106 cells/mL. The concentration was measured using a Neubauer chamber. For photodynamic inactivation, the standard suspension of the compound at a concentration of 12.5 mM (concentration defined in the cytotoxicity test previously described) was tested for evaluating the yeast killing. The absorption spectrum of the *cis*-[Ru(phen)$_2$(pPDI)]$^{2+}$ was determined by UV–vis spectroscopy. According to the experimental conditions, 0.1 mL of the *C. albicans* suspension was added to each well of a 96-well flat bottom microtiter plate (Costar Corning, New York, USA) with an area of 0.38 cm^2. Next, the P+L+ and P+L− groups (P = photosensitizer, L = light) received 0.1 mL of the *cis*-[Ru(phen)$_2$(pPDI)]$^{2+}$ solution. For the P−L+ and P−L− groups, 0.1 mL of physiological solution was added. For control methanol group 0,1 mL of methanol was added. The plates were shaken for 5 min (pre-irradiation time) in an orbital shaker (Solab, Piracicaba, Brazil). Next, each well of the groups submitted to the *cis*-[Ru(phen)$_2$(pPDI)]$^{2+}$ and LED and the P−L+ group were irradiated separately. A green LED (MMOptics, São Carlos, Brazil) with a wavelength of 532 ± 10 nm, output power of 90 mW, fluency of 42.63 J cm^2 (energy of 16.2 J and area of 0.38), time of 180 s, and fluency rate of 237 mW cm^2 was used for irradiation. The irradiation was performed under aseptic conditions in a laminar flow hood protected from light. A matte black screen with a hole whose diameter corresponded to the size of the well entrance was used to prevent the scattering of light. After irradiation, serial dilutions were prepared and 0.1-mL aliquots were spread on Sabouraud dextrose agar plates in duplicate. The plates were incubated at 37 °C for 48 h. After incubation, the number of colonies forming units per milliliter (CFU/mL) was determined and the results were log transformed.

2.4. Computational methods

All calculations were performed with the Gaussian 09 (G09) program package [34,35], edition D.01, employing the DFT method with Becke's three-parameter hybrid functionaly and Lee-Yang-Parr's gradient corrected correlation functional [35–37] (B3LYP) in combination with LanL2DZ basis set [37]. The ground-state geometries of the complexes were optimized in the gas phase. SCF-tight convergence criteria were used for all optimizations. The solvent DMSO was included in the calculations using the PCM system. The triplet state was obtained using UB3LYP/LANL2DZ. Electronic analysis was performed using TD-DFT calculations with 40 excited states.

3. Results and discussion

3.1. Synthesis and characterization

3.1.1. Structural and optical characterization

Our attempts to grow diffraction-quality crystals of the synthesized free ligand (pPDI) and of the Ru complex were not successful. We therefore determined the structural parameters and electronic effects on the coordination of the pPDI to the *cis*-[Ru(phen)$_2$] with DFT calculations. Fig. 2 shows the optimized structure for pPDI and *cis*-[Ru(phen)$_2$(pPDI)]$^{2+}$. The vibrational modes were obtained ensuring that imaginary frequencies were not generated in the minimum structures. The good agreement between the absorption and infrared theoretical and experimental data are discussed below.

The optimized structure of the substituted perylene ligand shows that the perylene moiety is perpendicular to the phenanthroline ligand, and the predicted dihedral angle between the phenanthroline and the perylene is 89.8°. After coordination of the pPDI ligand to the Ru(II) moiety, no pronounced changes are observed in the bond lengths and angles of the pPDI ligand. The most noticeable difference is the slight decrease in the perpendicularity of the phen-perylene ligand, as the dihedral angle in the complex is 85.6°. These changes do not affect the orbital composition indicating that the emissive properties of the pPDI will be not affected by the coordination to the metal complex.

3.1.2. IR spectra

The experimental IR spectra for the free pPDI and for the complex *cis*-[Ru(phen)2(pPDI)](PF6)2 (Fig. S3-Supporting information) exhibit stretching bands consistent with the proposed structures [38]. For the pPDI the absorption band at 1766 cm^{-1} refers to the carbonyl anhydride stretch and the bands at 1703 and 1666 cm^{-1} correspond to the stretches of the imide group νC—O [11,12,22,38].

The band at 1029 cm^{-1} refers to νC—O—C of the anhydride and at 1358 cm^{-1} corresponds to the C—N amine formed by the replacement of the oxygen atom of the anhydride by the nitrogen of phenanthroline, showing that phenanthroline was functionalized in only one Perylene side [39]. For the [Ru(phen)$_2$(pPDI)](PF$_6$)$_2$ complex the bands are shown at 1705, 1659 and 1359 cm^{-1} attributed to the stretches of the imide and imine groups (ν_{CO} and ν_{CN}), respectively [39]. The bands observed at 860 and 557 cm^{-1}, are assigned to the P-F stretch from the PF_6^-, [11]. In the theoretical spectrum for both the pPDI and Ru complex (Figs. S4 and S5 - Supporting information), the vibrational modes of the imine and imide groups are found at 1707, 1633, 1606 and 1339 cm^{-1}. The presence of a more intense band at 1339 cm^{-1} and also the appearance of the Ru-N stretching at 400–700 cm^{-1} in the measured spectrum are present after the coordination of the pPDI to the Ru-complex.

3.1.3. Cyclic voltametry

The electrochemical behavior of the complex *cis*-[Ru(phen)2(pPDI)]$^{2+}$ was investigated by cyclic voltammetry in order to evaluate the effect of the metal coordination on the reductive and oxidative potentials. The cyclic voltammogram of the complex in CH_3CN solution using a Pt electrode at the scanning rate of 100 mV s^{-1} is shown in Fig. 3. Using the data from the voltammetric curves, we identified the redox pairs at −0.25/-0.04 V, ($E^1/_2$ = −0.15 V) and −0.65/-0.39 V ($E^1/_2$ = −0.52 V) *vs* Ag+/AgCl, which were assigned to the anionic (pPDI/pPDI$^{\bullet-}$) and dianion radicals (pPDI$^{\bullet-}$/pPDI^{-2}) moieties of the *cis*-[Ru(phen)2(pPDI)]$^{2+}$ respectively, as reported for other perylene derivatives [20,22,40,41]. The electrochemical reductive process at −1.07 V and −1.22/-1.07 V ($E^1/_2$ = −1.15 V) were assigned to the phenanthroline ligand coordinated to the metal center Ru(II).

At 100 mV s^{-1}, the irreversible oxidative process at 1.17 V *vs* Ag+/AgCl was assigned to species Ru(II) → Ru(III) [11,38,41]. This oxidation potential is much higher than that observed for the precursor *cis*-RuCl$_2$(1,10-phen)$_2$, +0.43/+0.35 V (ΔE = 60 mV), probably because of the electron withdrawing character of the perylene group, which makes the metal center more electron-deficient.

3.1.4. Ground state absorption and luminescence

Since the free pPDI showed low solubility in CH_3CN, the absorption spectrum was obtained using diluted DMSO solutions (1.1×10^{-6} mol l^{-1}), as seen in Fig. 4.

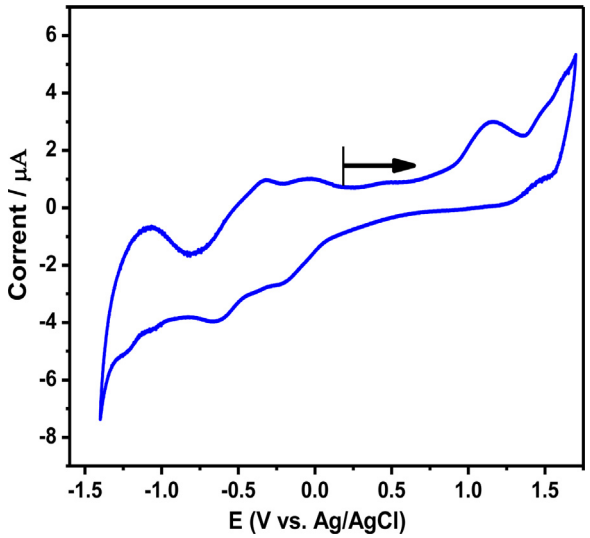

Fig. 3. Cyclic voltammogram of cis-[Ru(phen)$_2$(pPDI)]$^{2+}$ complex in acetonitrile (0.1 M) ($nBu)_4NPF_6$, platinum working electrode, (potential versus Ag/AgCl) and scan rate of 100 mV s^{-1}. $E_{1/2}$ for Fc^+/Fc couple = +0.54 V measured under the same experimental conditions.

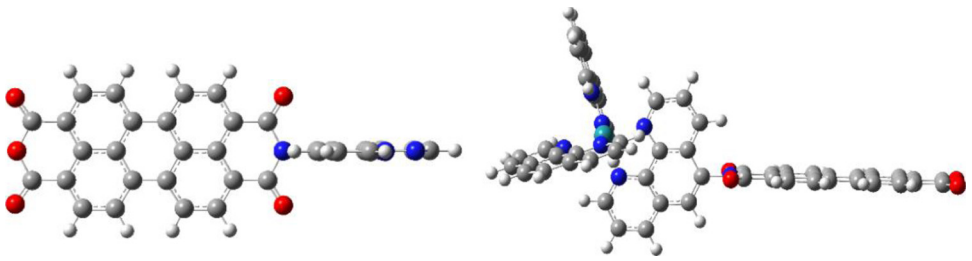

Fig. 2. DFT optimized structure of ligand pPDI [22] and *cis*-[Ru(phen)$_2$(pPDI)]$^{2+}$.

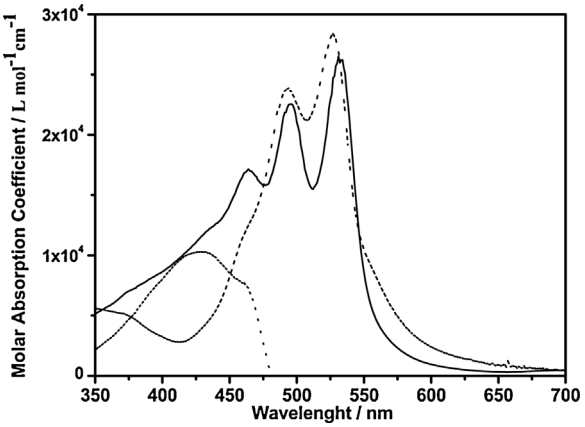

Fig. 4. UV–vis absorption spectrum (solid) of a 5.0×10^{-6} mol L^{-1} solution of *cis*-[Ru (phen)$_2$(pPDI)](PF$_6$)$_2$ in DMSO and the contributions of the free pPDI also in DMSO (short dash) and {Ru(phen)$_3$}$^{2+}$ MLCT absorption (dot) bands.

The UV–vis spectrum of pPDI exhibits a broad band with a shoulder at 555 nm and three distinct maxima at 533 nm, 493 nm, and 462 nm attributed to the π-π* electronic transitions of the perylene [11,22,39–41]. The electronic spectrum of the complex *cis*-[Ru(phen)$_2$(pPDI)]$^{2+}$ as seen in Fig. 3 exhibits transitions characteristic of the free pPDI along with the broad absorption band assigned as a MLCT of the complex [Ru(phen)3]$^{2+}$, with the maximum absorption at ~450 nm.

The theoretical electronic spectrum of the pPDI ligand shows a band at λ_{max} = 555 nm assigned to $\pi_{pery} \rightarrow \pi^*_{pery}$ transition (100% HOMO → LUMO) located completely on the perylene ring [22]. For the complex *cis*-[Ru(phen)$_2$(pPDI)]$^{2+}$ the theoretical electronic spectrum (Fig. S6- Supporting information) has a band at 556 nm due to the $\pi_{pery} \rightarrow \pi^*_{pery}$ transition of the perylene ligand (100% HOMO–3 → LUMO) and the transition at 447 nm caused by MLCT $d_{Ru} \rightarrow \pi^*_{phen}$ (43% HOMO–2 → LUMO + 1), as shown in Fig. 5.

The absorption bands of the *cis*-[Ru(phen)$_2$(pPDI)]$^{2+}$ did not change significantly relative to those of free pPDI. This observation is related to the fact that the pPDI moiety and the Ru metal center are in different nodal plans, a characteristic that has also been observed in other polypyridine complexes of Ru with aromatic chromophores [11,39,42]. This indicates that the complex does not behave as a conjugated super-molecule, but rather as an electron receptor-donor dyad.

The shape of the fluorescence spectra of *cis*-[Ru(phen)$_2$(pPDI)]$^{2+}$ is characteristic of the free perylene emission [10,11,13,16,22,43]. To study the effect of the perylene chromophore on polypyridine complexes, the compounds were excited at three different wavelengths (413 nm, 460 nm and 495 nm). Upon excitation at 413 nm, the complex exhibits a broad emission band (Fig. 6A). When excited at the 460 nm and 495 nm lengths (Fig. 6B and C, respectively), we observed that the complex exhibits a broadband with maximum at 550 nm and three distinct peaks, assigned the ILCT transitions of the perylene group with λ_{max} at 550, 584, and 635 nm, related to (0 ← 0), (0 ← 1) and (0 ← 2), respectively, suggesting a different distribution of the excitation light between the molecules {Ru(phen)3}$^{2+}$ and the free pPDI at each excitation length.

In agreement with these results, the excitation spectra obtained at 460 nm and 600 nm show two overlapping absorption bands characteristic of the {pPDI} and {Ru(phen)$_3$}$^{2+}$ moieties.

The approximate mirror-image relation between the absorption and fluorescence bands at 460 nm and 490 nm are caused by relatively small differences between the geometry of the ground S_0 and excited singlet state S_1, which are typical for the rigidity and planarity of the polycyclic aromatic molecules [17,22,42].

These results were confirmed by the time-resolved luminescence decays of air equilibrated dilute solutions of the complex *cis*-[Ru(phen)$_2$(pPDI)]$^{2+}$ in CH_3CN and the free pPDI in DMSO solutions (Figs. S7 and S8 - Supporting information). When excited in the absorption region of the MLCT transition (445 nm), both the {Ru(phen)$_2$}$^{2+}$ and the {pPDI} moieties are electronically excited. The complex *cis*-[Ru(phen)$_2$(pPDI)]$^{2+}$ showed a bi-exponential behavior with lifetimes of 5.06 ns (48.1%) and 156 ns (51.9%), resulting from pPDI and ^{3}MLCT emission, respectively. By excitation at 532 nm, the *cis*-[Ru(phen)$_2$(pPDI)]$^{2+}$ showed a bi-exponential behavior with lifetime of 0.60 ns (1.27%) and 4.25 ns (98.73%) caused by pPDI emission, consistent with the lifetime of 4.83 ns observed for the free ligand.

The emission from the free pPDI exhibited a bi-exponential behavior when λ_{exc} = 515 nm with λ_{em} = 550 nm. Kirmaie and co-workers [44] suggested that a lifetime on the order of 1 ns in the perylene dye emission is related to the fluorescence via molecular vibrations. The longer lifetime (on the order of 5 ns) is attributed to the transition $S_0 \leftarrow S_1$ [41,42]. After coordination to the metal ion, the emission with the shortest lifetime can no longer be detected.

Excitation in the visible region will ultimately lead to intersystem crossing and population of the lowest energy ^{3}MLCT state. Indeed, the orbital composition for the lowest triplet state optimized structure shows that the HOMO is mainly composed of perylene and the LUMO by Ru-phen moiety. The spin density distribution for the triplet optimized structure is completely located on the perylene ligand, Fig. 7.

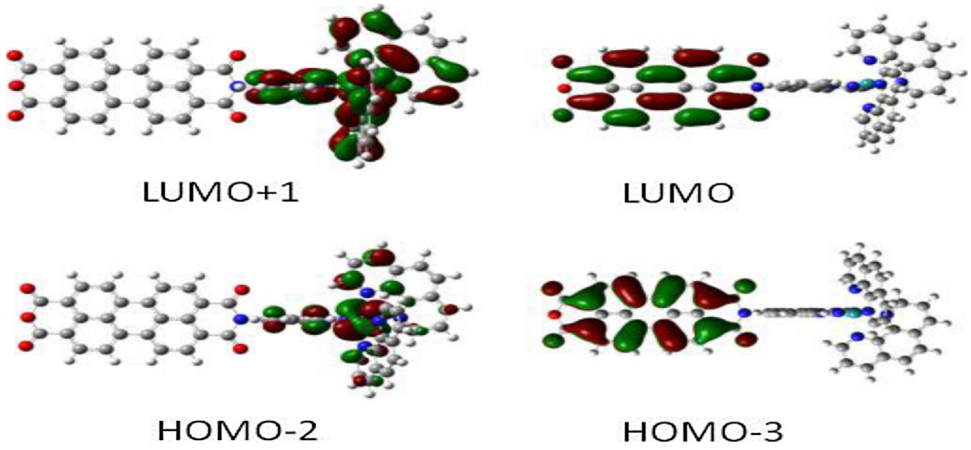

Fig. 5. Contour surfaces for the HOMOs and LUMOs orbitals of the *cis*-[Ru(phen)$_2$(pPDI)]$^{2+}$.

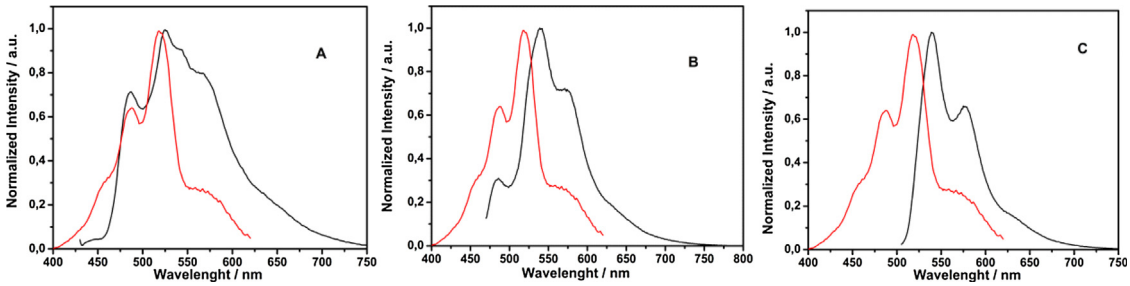

Fig. 6. Luminescence spectra (black) of the cis-$[Ru(phen)_2(pPDI)]^{2+}$ by excitation at λ_{exc} = 413 nm (A), λ_{exc} = 460 nm (B) and λ_{exc} = 495 nm (C) and excitation spectra (red) recorded at λ_{em} = 620 nm in DMSO. (For interpretation of the references to colour in this figure legend, the reader is referred to the web version of this article.)

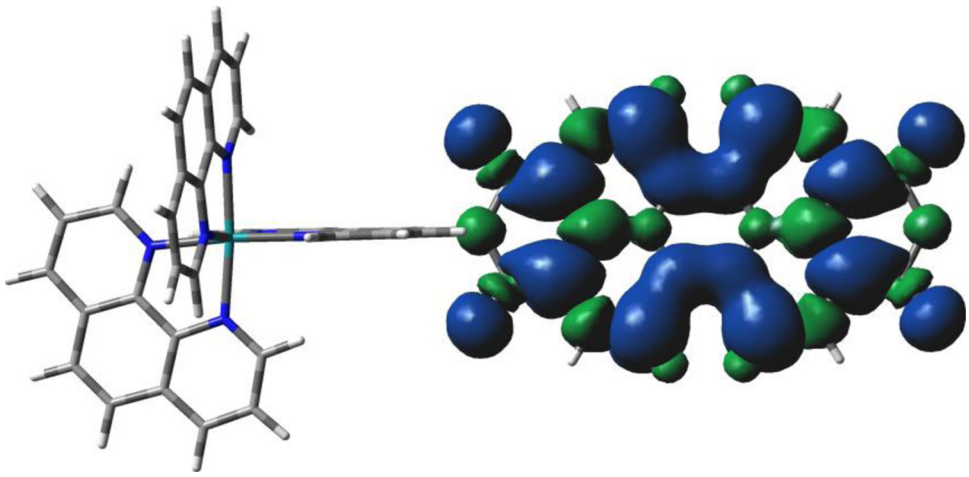

Fig. 7. Spin density distribution in the geometry optimized ^{3}MLCT of compound *cis*-$[Ru(phen)_2(pPDI)]^{2+}$.

TD-DFT vertical excitation revealed that the T_2 and S_1 levels of the compound *cis*-$[Ru(phen)_2(pPDI)]^{2+}$ are degenerate (1.88 eV) and very close in energy to the T_3 and S_2 (2.0 eV) levels which are degenerate as well. T_2 and S_1 are characterized by $Ru \rightarrow \pi^*_{pery}$ charge transfer and T_3 and S_2 by the $\pi_{pery} \rightarrow \pi^*_{pery}$ transition.

3.2. Singlet oxygen measurements – efficiency of singlet oxygen photogeneration

Although PDIs are known as dyes with high fluorescence quantum yields, a number of transition-metal complexes of PDI dyes were recently reported to accelerate intersystem crossing (ISC) from singlet to triplet-excited state. As a consequence, under aerobic conditions, formation of $^1O_2$ is possible [14,40,43,44]. Therefore, we investigated formation of $^1O_2$ from our compounds upon light irradiation. $^1O_2$ quantum yields were evaluated for the complex by using the direct observation of the near infrared (NIR) singlet oxygen emission signal.

The quantum yield of singlet oxygen production by *cis*-$[Ru(phen)_2(pPDI)]^{2+}$ was measured in dichloromethane, chloroform, and acetonitrile. Methylene blue was used as the reference sensitizer. The free ligand pPDI did not show any singlet oxygen production. On the other hand, the complex *cis*-$[Ru(phen)_2(pPDI)]^{2+}$ does generate singlet oxygen with moderate efficiency; the quantum yields of singlet oxygen generation in different solvents are given in Table 1. All measurements were made in triplicates. It is striking that the quantum yields do not vary much across solvents with different dielectric constants. This indicates that singlet oxygen generation via charge-transfer intermediates is probably not a significant pathway for this complex.

Table 1
Quantum yields of singlet oxygen measured upon irradiation at 532 nm for complex 1 in different deuterated organic solvents.

Solvent	$\Phi\Delta$ *cis*-$[Ru(phen)_2(pPDI)]^{2+}$	Φ_Δ Methylene Blue
[c,d] dichloromethane	0.24 ± 0.005	0.57
[c,d] methanol-d4	0.23 ± 0.06	0.58[6,7]
[a,b] acetonitrile-d3	0.26 ± 0.005	0.57[7,10,13]
[c,d] acetonitrile	0.24 ± 0.002	0.52
[a,d] chloroform	0.18 ± 0.006	0.52, [10,13]

The measurements were made in triplicates. Error is given as one standard deviation.
[a] Saturated atmosphere O_2.
[b] Deuterated solvent.
[c] Air saturated atmosphere.
[d] Anhydrous solvent.

The ability to produce singlet oxygen depends largely on the production of a long-lived triplet state, [13,14,17,18] and the moderate quantum yield values of $^1O_2$ and the high absorbance of the perylene moiety in the visible range make *cis*-$[Ru(phen)_2(pPDI)]^{2+}$ a possible photosensitizer to be used in water disinfection or other singlet oxygen-base processes that use sunlight as an excitation source. Since the Ru complex has a long-lived triplet state, it is of possible that in addition to formation of singlet oxygen, formation of superoxide anion by electron-transfer processes and/or Type I photooxidation processes take place upon irradiation of the Ru complex under aerobic conditions. The reactive oxygen species resulting from these processes may

also be involved in the fungicidal processes described in Sections 3.3 and 3.4 below.

3.3. Cytotoxicity assays of the PSs in mouse macrophages

The cytotoxicity tests were performed in order to obtain the concentration of the *cis*-[Ru(phen)$_2$(pPDI)]$^{2+}$ complex (without irradiation) that has low cytotoxicity, as we are interested in observing the toxicity from singlet oxygen.

The photosensitizer showed high cytotoxicity at concentrations above 25 μM. The concentrations of 12.5 μM and 6.25 μM were the concentrations that presented low cytotoxicity represented by high cell viability (Fig. 8). For the subsequent test the concentration of 12.5 μM was selected, since this concentration showed low cytotoxicity in comparison to the higher concentrations.

3.4. Photodynamic inactivation assays for Candida albicans

After observing the light-dependent $^1O_2$ production by complex *cis*-[Ru(phen)$_2$(pPDI)]$^{2+}$, and their effect on mouse macrophages cultures, these systems were tested as active components in antimicrobial photodynamic therapy. Owing to its medical importance, *C. albicans* was chosen as the model microorganism. The viability of these cells as a function of different exposure, and different conditions during the experiments is shown in Fig. 9.

For the photodynamic therapy (PDT) test, we used the concentration of the photosensitizer of 12.5 μM, as that was the concentration that presented low cytotoxicity represented by high macrophages cells viability in previous test described (Cytotoxicity Assay).

We observed that the group that was exposed only to the photosensitizer (no irradtion, P+L-) presented a statistically significant reduction of *C. albicans* when compared to the P-L- and P-L+ control groups ($p = 0.0053$ and $p = 0.0030$). There was no statistical difference when these groups (P-L- and P-L+) was compared to the methanol group ($p = 0.1764$), indicating that the photosensitizer, independent of the methanol activity, had fungicidal action on *C. albicans* cells. Regarding the PDT group (P + L +), we observed that this group showed by far the most inhibitory action on *C. albicans* in comparison with all the other experimental groups ($p < 0.0001$).

Freire et al. in 2013 [33] studied the ability of Rose Bengal (RB) and Eosin Y (2,4,5,7 tetrabromofluorescein) for photoinactivation in *C. albicans*. These authors used the *C. albicans* biofilm formation

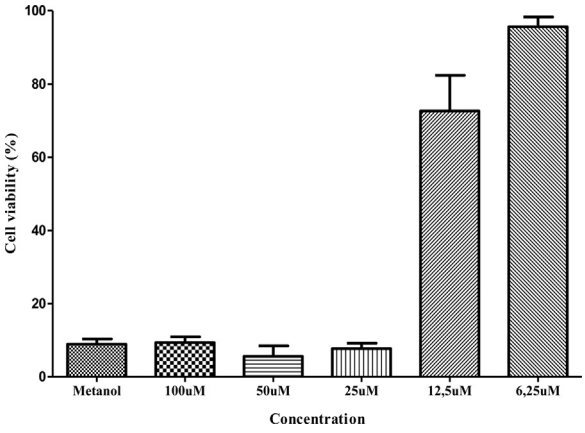

Fig. 8. Percentage average and standard deviation of cell viability of macrophages RAW 265.7 exposed to different concentrations of the photosensitizer *cis*-[Ru(phen)$_2$(pPDI)]$^{2+}$.

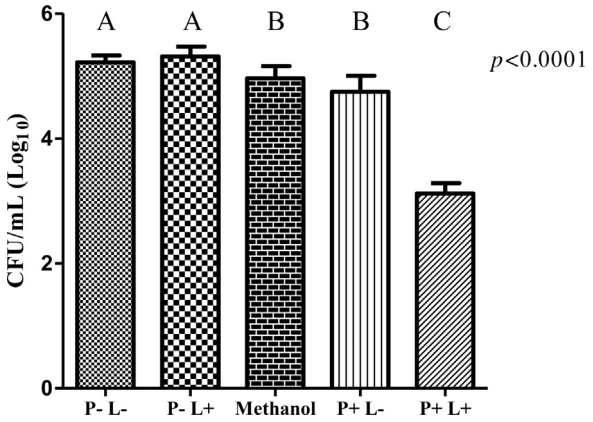

Fig. 9. Colony-forming units (CFU/mL) of *C. albicans* average and standard deviation after different treatments with the photosensitizer *cis*-[Ru(phen)$_2$(pPDI)]$^{2+}$. Experimental groups: P + L+ photosensitizer and light irradiation, P + L− only treated with the photosensitizer, P−L+ only light irradiation, P−L− control group not submitted to the photosensitizer or light irradiation, methanol is the control group of this solvent.

for evaluation. After treatment with RB 200 μM or Eosin Y, inactivation rates of 0.22 and 0.45 log$_{10}$ were observed for RB and Eosin Y, respectively. In our study, the PDT (P + L +) with the compound and light showed significant log reduction (2.09 log$_{10}$) expressed in CFU/ml of *C. albicans*, as described above. The organization in biofilm allows a greater resistance of the microorganisms against antimicrobial agents than the planktonic cells organization. In our study, we have established that a there is a significant antimicrobial effect of *cis*-[Ru(phen)$_2$(pPDI)]^2 and a considerable rate of microbial reduction at low concentrations of the photosensitizer. For example, we obtained reduction of 2.09 log$_{10}$ at a concentration of 12.5 μM of this photosensitizer, while Peloi et al., 2008 [45] using a methylene blue concentration of 35.2 μM observed a reduction of 2.77-3.87 log$_{10}$.

4. Conclusion

We have successfully prepared and characterized new perylene derivatives and a *cis*-[Ru(phen)$_2$(pPDI)]$^{2+}$ complex in which a perylene moiety has been attached to one of the ligands. “The optimized structure of the new substituted perylene ligand shows that the perylene moiety is perpendicular to the phenanthroline ligand. After coordination of the pPDI ligand to the Ru(II) moiety, no pronounced changes are observed in the bond lengths and angles of the pPDI ligand. The coordination does not affect the orbital make-up, indicating that the emissive properties of the pPDI are not affected by the coordination to the metal complex. In addition, the absorption bands and the shape of the fluorescence spectra of the *cis*-[Ru(phen)$_2$(pPDI)]$^{2+}$ did not change significantly relative to those of free pPDI. These observation is consistent with the pPDI moiety and the Ru metal center being in different nodal plans.”

Upon irradiation in the visible range, the latter Ru complex does produce singlet oxygen. The photosensitizer diluted in methanol to a concentration of 12.5 μM presents lower cytotoxicity compared to the others concentrations of this compound and, this photosensitizer can statistically inhibit *C. albicans* cells. Despite the modest singlet oxygen quantum yield, the high molar absorptivity of the perylene ligand makes our system a possible agent for photodynamic therapy against *C. albicans*. Our results demonstrate the potential use of such Ru metal complexes for fungicidal photodynamic therapy against *C. albicans*.

Acknowledgements

The authors would like to acknowledge FAPESP, (process n°. 2012/09449-8 and 2014/17476-0), CNPq, and CAPES for the grants and fellowships received. The authors are indebted to D.Z. and M.S. gratefully acknowledges support from the NSF-CREST program (NSF-HRD 1547723).

Appendix A. Supplementary data

Supplementary data associated with this article can be found, in the online version, at https://doi.org/10.1016/j.jphotochem.2017.12.020.

References

[1] C. Schweitzer, R. Schmidt, Physical mechanisms of generation and deactivation of singlet oxygen, Chem. Rev. 103 (2003) 1685–1758, doi:http://dx.doi.org/10.1021/cr010371d.
[2] D. Ashen-Garry, M. Selke, Singlet oxygen generation by cyclometalated complexes and applications, Photochem. Photobiol. 90 (2014) 257–274, doi:http://dx.doi.org/10.1111/php.12211.
[3] F. Doria, I. Manet, V. Grande, S. Monti, M. Freccero, Water-soluble naphthalene diimides as singlet oxygen sensitizers, J. Org. Chem. 78 (2013) 8065–8073, doi:http://dx.doi.org/10.1021/jo401347z.
[4] V. Prusakova, C.E. McCusker, F.N. Castellano, Ligand-localized triplet-state photophysics in a platinum(II) terpyridyl perylenediimideacetylide, Inorg. Chem. 51 (2012) 8589–8598, doi:http://dx.doi.org/10.1021/ic301169t.
[5] B. Bruner, M.B. Walker, M.M. Ghimire, D. Zhang, M. Selke, K.K. Klausmeyer, M. A. Omary, P.J. Farmer, Ligand-based photooxidations of dithiomaltolato complexes of Ru(II) and Zn(II): photolytic CH activation and evidence of singlet oxygen generation and quenching, Dalton Trans. 43 (2014) 11548–11556, doi:http://dx.doi.org/10.1039/c4dt00961d.
[6] A.A. Abdel-Shafi, H.A. Hassanin, S.S. Al-Shihry, Partial charge transfer contribution to the solvent isotope effect and photosensitized generation of singlet oxygen, O2Δ1(g), by substituted ruthenium(II) bipyridyl complexes in aqueous media, Photochem. Photobiol. Sci. 13 (2014) 1330–1337, doi:http://dx.doi.org/10.1039/c4pp00117f.
[7] A.A. Abdel-Shafi, D.R. Worrall, A.Y. Ershov, Photosensitized generation of singlet oxygen from ruthenium(ii) and osmium(ii) bipyridyl complexes, Dalt. Trans. 103 (2004) 30–36, doi:http://dx.doi.org/10.1039/b310238f.
[8] J.N. Demas, E.W. Harris, R.P. McBride, Energy transfer from luminescent transition metal complexes to oxygen, J. Am. Chem. Soc. 99 (1977) 3547–3551, doi:http://dx.doi.org/10.1021/ja00453a001.
[9] T.Q. Ni, L.A. Melton, Non-radiative PII-, 67 (1992).
[10] D. Garcìa-Fresnadillo, Y. Georgiadou, G. Orellana, A.M. Braun, E. Oliveros, Singlet-Oxygen (1Δg) Production by Ruthenium(II) complexes containing polyazaheterocyclic ligands in methanol and in water, Helv. Chim. Acta 79 (1996) 1222–1238, doi:http://dx.doi.org/10.1002/hlca.19960790428.
[11] E.R.D. Santos, J. Pina, T. Venâncio, C. Serpa, J.M.G. Martinho, R.M. Carlos, Photoinduced energy and electron-Transfer reactions by polypyridine ruthenium(II) complexes containing a derivatized perylene diimide, J. Phys. Chem. C 120 (2016) 22831–22843, doi:http://dx.doi.org/10.1021/acs.jpcc.6b06693.
[12] C. Mari, H. Huang, R. Rubbiani, M. Schulze, F. W??rthner, H. Chao, G. Gasser, Evaluation of perylene bisimide-based RuII and IrIII complexes as photosensitizers for photodynamic therapy, Eur. J. Inorg. Chem. 2017 (2017) 1745–1752, doi:http://dx.doi.org/10.1002/ejic.201600516.
[13] A.A. Abdel-shafi, P.D. Beer, R.J. Mortimer, F. Wilkinson, Photosensitized generation of singlet oxygen from vinyl linked benzo-crown-ether-bipyridyl ruthenium(II) complexes, J. Phys. Chem. A 104 (2000) 192–202, doi:http://dx.doi.org/10.1021/jp991876z.
[14] C. Girardot, G. Lemercier, J.C. Mulatier, C. Andraud, J. Chauvin, P.L. Baldeck, Novel 5-(oligofluorenyl)-1,10-phenanthroline type ligands: synthesis, linear and two-photon absorption properties, Tetrahedron Lett. 49 (2008) 1753–1758, doi:http://dx.doi.org/10.1016/j.tetlet.2008.01.080.
[15] J. Moreau, F. Lux, M. Four, J. Olesiak-Banska, K. Matczyszyn, P. Perriat, C. Frochot, P. Arnoux, O. Tillement, M. Samoc, G. Ponterini, S. Roux, G. Lemercier, A 5-(difluorenyl)-1,10-phenanthroline-based Ru(II) complex as a coating agent for potential multifunctional gold nanoparticles, Phys. Chem. Chem. Phys. 16 (2014) 14826–14833, doi:http://dx.doi.org/10.1039/c4cp01534g.
[16] G.T.P. Brancini, G.B. Rodrigues, M. de S.L. Rambaldi, C. Izumi, A.P. Yatsuda, M. Wainwright, J.C. Rosa, G.Ú.L. Braga, The effects of photodynamic treatment with new methylene blue N on the Candida albicans proteome, Photochem. Photobiol. Sci. 15 (2016) 1503–1513, doi:http://dx.doi.org/10.1039/C6PP00257A.
[17] Y.S. El-Sayed, S.A. El-Daly, 3,4,9,10-Perylenetetracarboxylic acid derivatives, their spectral behavior and their chemical interaction with hydrated iron oxide nanopar, Chin. J. Chem. 28 (2010) 363–370, doi:http://dx.doi.org/10.1002/cjoc.201090080.
[18] Z. Yu, Y. Wu, Q. Peng, C. Sun, J. Chen, J. Yao, H. Fu, Accessing the triplet state in heavy-atom-free perylene diimides, Chem.—A Eur. J. 22 (2016) 4717–4722, doi:http://dx.doi.org/10.1002/chem.201600300.
[19] H. Langhals, R. Ismael, Cyclophanes as model compounds for permanent, dynamic aggregates—induced chirality with strong CD effects, Eur. J. Org. Chem. (1998) 1915–1917, doi:http://dx.doi.org/10.1002/(SICI)1099-0690(199809)1998:9<1915:AID-EJOC1915>3.0.CO;2-1.
[20] P. Maia, E. Medeiros, B. Maria, L. Vega, H. Nunes, F.A. de Freitas, Synthesis and characterization of a perylene derivative and its application as catalyst for ethanol electro—oxidation, Chem. Pap. (2017), doi:http://dx.doi.org/10.1007/s11696-017-0344-z.
[21] H. Langhals, carboxylic imide structures as structure elements of high stability. Novel developments in perylene dye chemistry, Heterocycles 40 (1995) 477–500, doi:http://dx.doi.org/10.3987/REV-94-SR2.
[22] P.J.S. Maia, Synthesis, Spectroscopic Characterization, Photophysical Properties of N,-(5-amin-1, 10-phenanthroline) perylene-3, 4, 9, 10-tetracarboximonoimide, IOSR Journal of Applied Chemistry 10 (2017) 13–20.
[23] M.T. Rawls, J. Johnson, B.A. Gregg, Coupling one electron photoprocesses to multielectron catalysts: towards a photoelectrocatalytic system, J. Electroanal. Chem. 650 (2010) 10–15, doi:http://dx.doi.org/10.1016/j.jelechem.2010.09.016.
[24] F. Yukruk, A.L. Dogan, H. Canpinar, D. Guc, E.U. Akkaya, Water-soluble green perylenediimide (PDI) dyes as potential sensitizers for photodynamic therapy, Org. Lett. 7 (2005) 2885–2887, doi:http://dx.doi.org/10.1021/ol050841g.
[25] I.T. Kato, R.A. Prates, C.P. Sabino, B.B. Fuchs, G.P. Tegos, E. Mylonakis, M.R. Hamblin, M.S. Ribeiro, Antimicrobial photodynamic inactivation inhibits Candida albicans virulence factors and reduces in vivo pathogenicity, Antimicrob. Agents Chemother. 57 (2013) 445–451, doi:http://dx.doi.org/10.1128/AAC.01451-12.
[26] B.M. Soares, D.L. da Silva, G.R. Sousa, J.C.F. Amorim, M.A. de Resende, M. Pinotti, P.S. Cisalpino, In vitro photodynamic inactivation of Candida spp. growth and adhesion to buccal epithelial cells, J. Photochem. Photobiol. B Biol. 94 (2009) 65–70, doi:http://dx.doi.org/10.1016/j.jphotobiol.2008.07.013.
[27] M. Wainwright, T. Maisch, S. Nonell, K. Plaetzer, A. Almeida, G.P. Tegos, M.R. Hamblin, Photoantimicrobials—are we afraid of the light? Lancet Infect. Dis. 17 (2017) e49–e55, doi:http://dx.doi.org/10.1016/S1473-3099(16)30268-7.
[28] L.P. Brion, S.E. Uko, D.L. Goldman, Risk of resistance associated with fluconazole prophylaxis: systematic review, J. Infect. 54 (2007) 521–529, doi:http://dx.doi.org/10.1016/j.jinf.2006.11.017.
[29] T. Abduljabbar, M. Al-Askar, M.K. Baig, Z.H. AlSowygh, S.V. Kellesarian, F. Vohra, Efficacy of photodynamic therapy in the inactivation of oral fungal colonization among cigarette smokers and non-smokers with denture stomatitis, Photodiagnosis Photodyn. Ther. 18 (2017) 50–53, doi:http://dx.doi.org/10.1016/j.pdpdt.2017.01.182.
[30] B.P. Sullivan, D.J. Salmon, T.J. Meyer, Mixed phosphine 2,2'-Bipyridine complexes of ruthenium, Inorg. Chem. 17 (1978) 3334–3341, doi:http://dx.doi.org/10.1021/ic50190a006.
[31] E.C. Johnson, B.P. Sullivan, D.J. Salmon, S.A. Adeyemi, T.J. Meyer, Synthesis and properties of the chloro-bridged dimer [(bpy)2RuCl]22+ and its transient 3+ mixed-valence ion, Inorg. Chem. 17 (1978) 2211–2215, doi:http://dx.doi.org/10.1021/ic50186a038.
[32] J. Rafael De Oliveira, V. Carlos De Castro, P. Das, G. Figueiredo Vilela, S. Esteves, A. Camargo, C. Antonio, T. Carvalho, A. Olavo, C. Jorge, L. Dias De Oliveira, Cytotoxicity of Brazilian plant extracts against oral microorganisms of interest to dentistry, BMC Complement. Altern. Med. 13 (2013) 1, doi:http://dx.doi.org/10.1186/1472-6882-13-208.
[33] F. Freire, A.C.B.P. Costa, C.A. Pereira, M. Beltrame, J.C. Junqueira, A.O.C. Jorge, Comparison of the effect of rose bengal- and eosin Y-mediated photodynamic inactivation on planktonic cells and biofilms of Candida albicans, Lasers Med. Sci. 29 (2014) 949–955, doi:http://dx.doi.org/10.1007/s10103-013-1435-x.
[34] M.J. Frisch, G.W. Trucks, H.B. Schlegel, G.E. Scuseria, M.A. Robb, References [1], (2009) 2009.
[35] A.D. Becke, Density-functional thermochemistry. III. The role of exact exchange, J. Chem. Phys. 98 (1993) 5648–5652, doi:http://dx.doi.org/10.1063/1.464913.
[36] C. Lee, W. Yang, R.G. Parr, Development of the Colle-Salvetti correlation-energy formula into a functional of the electron density, Phys. Rev. B 37 (1988) 785–789, doi:http://dx.doi.org/10.1103/PhysRevB.37.785.
[37] P.J. Hay, W.R. Wadt, *Ab initio* effective core potentials for molecular calculations. Potentials for K to Au including the outermost core orbitals, J. Chem. Phys. 82 (1985) 299–310, doi:http://dx.doi.org/10.1063/1.448975.
[38] G. Schnurpfeil, J. Stark, D. Wöhrle, Syntheses of uncharged, positively and negatively charged 3,4,9,10-perylene-bis(dicarboximides), Dye. Pigm. 27 (1995) 339–350, doi:http://dx.doi.org/10.1016/0143-7208(94)00075-D.
[39] S. Asir, A.S. Demir, H. Icil, The synthesis of novel, unsymmetrically substituted, chiral naphthalene and perylene diimides: photophysical, electrochemical, chiroptical and intramolecular charge transfer properties, Dye. Pigm. 84 (2010) 1–13, doi:http://dx.doi.org/10.1016/j.dyepig.2009.04.014.
[40] D. Gosztola, M.P. Niemczyk, W. Svec, A.S. Lukas, M.R. Wasielewski, Excited doublet states of electrochemically generated aromatic imide and diimide radical anions, J. Phys. Chem. A 104 (2000) 6545–6551, doi:http://dx.doi.org/10.1021/jp000706f.
[41] R.K. Dubey, M. Niemi, K. Kaunisto, K. Stranius, A. Efimov, N.V. Tkachenko, H. Lemmetyinen, Excited-state interaction of red and green perylene diimides

with luminescent Ru(II) polypyridine complex, Inorg. Chem. 52 (2013) 9761–9773, doi:http://dx.doi.org/10.1021/ic400474b.
[42] A. Juris, V. Balzani, F. Barigelletti, S. Campagna, P. Belser, A. von Zelewsky, Ru(II) polypyridine complexes: photophysics, photochemistry, eletrochemistry, and chemiluminescence, Coord. Chem. Rev. 84 (1988) 85–277, doi:http://dx.doi.org/10.1016/0010-8545(88)80032-8.
[43] H. Dinalp, Z. Akar, C. Zafer, S. Li, Effect of side chain substituents on the electron injection abilities of unsymmetrical perylene diimide dyes, Dye. Pigm. 91 (2011) 182–191, doi:http://dx.doi.org/10.1016/j.dyepig.2011.03.022.
[44] C. Kirmaier, E. Hindin, J.K. Schwartz, I.Y. Sazanovich, J.R. Diers, K. Muthukumaran, M. Taniguchi, D.F. Bocian, J.S. Lindsey, D. Holten, Synthesis and excited-state photodynamics of perylene-bis(imide)-oxochlorin dyads. A charge-separation motif, J. Phys. Chem. B 107 (2003) 3443–3454, doi:http://dx.doi.org/10.1021/jp0269423.
[45] Y. Suganuma, Y. Kowaka, N. Ashizawa, N. Nakayama, H. Goto, T. Ishimoto, U. Nagashima, T. Ueda, T. Yamanaka, N. Nishi, M. Baba, Mode-selective internal conversion of perylene, Mol. Phys. 109 (2011) 1831–1840, doi:http://dx.doi.org/10.1080/00268976.2011.593568.